1055-152 Quantitative High-Resolution Magnetic Resonance Imaging of an Atherosclerotic Rabbit Model With a Whole Body 1.5Tesla Magnetic Resonance Imaging System

Henning Steen, Joao A. Lima, Subroto Chatterjee, Rene Rodriguez, Hugo A. Katus, Matthias Stuber, Johns Hopkins Hospital, Baltimore, MD, Universitätsklinik, Klinik III, Heidelberg, Germany

Introduction:
High Resolution MRI for atherosclerotic vessel wall characterisation and quantification is hampered by low signal-and contrast to-noise ratio (SNR, CNR). We established an improved microscopic 3D MRI black-blood sequence for objective vessel SNR, -CNR and -sharpness analysis in a Watanabe model.
Methods:
Multiple subrenal ECG gated fatsat aortic 3D black blood Fast Spin Echo vessel wall images (TR=3 RR , TE=10.5ms, TI pre/post =400/300ms, FOV=76mm, in-plane resolution=0.25mm, phase encoding= Z direction) pre and 15 min. post contrast (Gad=0.1mmol/l) were investigated in 9 Watanabes (I=3 normals, II= 6 high cholesterol fed for 2 months) on a 1.5T MR system (Philips Medical). SNR-, CNR-, wall thickness and –sharpness- analysis were done semi-automatically pre-and post contrast using a two-tailed paired Student´s t-test.
Results:
High image quality (11min/scan) could be obtained in all animals (Fig 1). In I, SNR increased 30%, CNR 70 %. In II, SNR enhanced 297%, CNR 318%, (all p<0.05) with insignificant increases in vessel wall thickness post contrast in I and II. Vessel sharpness increase for I and II was similar (55% and 58%).
Discussion:
High quality aortic vessel wall images with dramatic increases of SNR and CNR post contrast can routinely be obtained which could be invested for superior spatial resolution to improve image quality in plaque characterization. Quantitative analysis software proves valuable for objective assessment of atherosclerotic parameters in vessel wall disease.

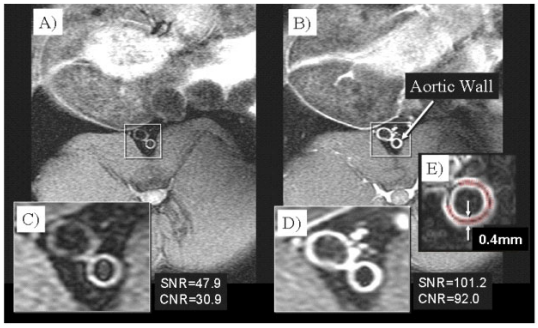

Figure 1 Delayed hyperenhancement in an atherosclerotic (Watanabe) rabbit model. A) pre-contrast with magnified version in C). B) & D) (magnified version) display the same delayed hyperenhanced section 15min post Gd injection with a substantially increased vessel-wall SNR and CNR. The vessel wall thickness as measured with the 'Soap-Bubble' analysis software (E) is 0.4mm.

1055-153 Effect of Contrast Enhancement on Measurement of Carotid Arterial Lumen and Wall Volume Using Magnetic Resonance Imaging

Binh An P. Phan, Baocheng Chu, Xue-Qiao Zhao, University of Washington, Seattle, WA

Background: Recent developments of contrast-enhanced (CE) magnetic resonance imaging (MRI) appear to be useful in detecting neovasculature, possibly related to inflammation, in carotid atherosclerotic plaques. We investigated the effect of gadolinium-based (GAD) CE on MRI measurements of lumen and wall volumes of carotid arteries.
Methods: Common carotid arteries (CCA) and internal carotid arteries (ICA) of 50 patients were imaged on a 1.5 T MRI. 10 quadruple inversion recovery T1-weighted images covering 20 mm of the CCA, bifurcation, and ICA were obtained before and after GAD administration. Quantitative measurements of carotid artery lumen and wall volume were performed using a semi-automated computer drawing program. Mean lumen and wall volume per artery before and after GAD were compared. The mean volume change due to CE between arteries with and without plaque involvement, and among levels of CCA, bifurcation, and ICA were also compared.
Results: The pre-CE volume, post-CE volume, and percent volume change for the lumen was 185.10 mm^3 ± 54.46, 177.52 mm^3 ± 50.21, and -3.73% ± 3.99, respectively. The pre-CE volume, post-CE volume, and percent volume change for the wall was 84.75 mm^3 ± 23.42, 108.67 mm^3 ± 27.9, and 30.57% ± 20.92, respectively. The published standard deviation (SD) on carotid measurement error using MRI is 6-10% for lumen and 11-12% for wall measurements. There was no significant difference in volume change due to CE in arteries with and without plaque involvement or among the levels of CCA, bifurcation, and ICA.
Conclusion: Gadolinium-based CE-MRI images showed a significant increase in wall volume in arteries with and without plaque involvement consistently throughout the CCA, bifurcation, and ICA. The observed increase in wall volume is greater than twice the published SD on wall measurement error using MRI. We hypothesize this increase in wall volume may be due to improved wall visibility, neovascularization, or endothelium dysfunction. The post-contrast wall volume increase should be taken into consideration in future CE-MRI studies of atherosclerotic plaque characteristics and especially in those studies evaluating plaque progression or regression.

1055-154 Magnetic Resonance Angiography Detects In-Stent Thrombosis and Thrombolysis

Min Su Hyon, Hideaki Kaneda, Fumiaki Ikeno, Krishna Nayak, Alan C. Yeung, Michael V. McConnell, Stanford University, Stanford, CA

Background: In-stent thrombosis is rare but life-threatening. In-vivo imaging of in-stent thrombus and its response to therapy would be beneficial. We evaluated MR angiography (MRA) for the detection of in-stent thrombosis and for monitoring of thrombolysis in a rabbit model.
Methods: Minimal-artifact copper stents (3.5-4.0mm x 6-14mm) were placed at infrarenal aorta in 16 New Zealand White rabbits. The stented aorta was imaged 1-4 days after stenting with 1.5T MRI system using: 1) a real-time MRA (20cm FOV, 1.1 x 1.1 x 5mm, 12-30f/s), 2) a "bright-blood" coronary MRA (16cm FOV, 20 interleaves, 0.58 x 0.58 x 3mm, TR=1000 ms, TE=7ms, flip angle=60°) and 3) a T1-weighted 3D "black-blood" SPGR with saturation slabs (TR 41ms, TE 4ms, flip angle=40°, 10cm FOV, 0.4 x 0.8 x 1.5mm). Thrombolysis using tPA (2mg/kg) was performed under monitoring with MRA. Animals were euthanized for confirmation of thrombi.
Results: In-stent thrombosis was detected in all by MRI. Histology confirmed the thrombi. The thrombus appeared as luminal irregularities in "bright-blood" sequence (A). In "black-blood" sequence, thrombus appeared as a more extensive ring along the stent as well as extending into the lumen (C). With thrombolysis, a marked decrease in in-stent thrombosis was demonstrated with both sequences (B, D) at 1-3 hours.
Conclusions: MRA can detect in-stent thrombosis and thrombolysis using a minimal-artifact stent. This is a promising noninvasive approach for studying arterial thrombosis and its response to treatment.

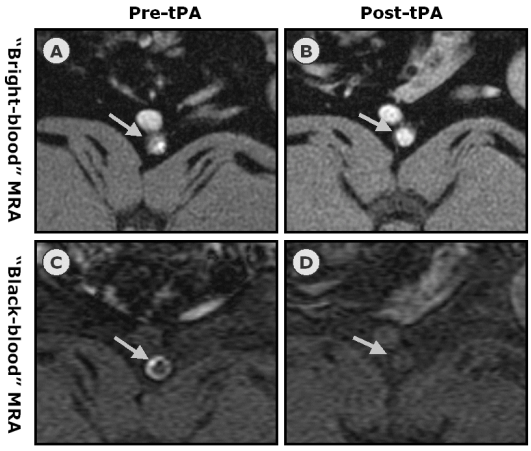

1055-155 Antiangiogenic Therapy of Early Atherosclerosis With Paramagnetic $\alpha_v\beta_3$-Integrin-Targeted Fumagillin Nanoparticles

Patrick M. Winter, Anne M. Morawski, Shelton D. Caruthers, Thomas D. Harris, Ralph W. Fuhrhop, Huiying Zhang, John S. Allen, Elizabeth K. Lacy, Todd A. Williams, Samuel A. Wickline, Gregory M. Lanza, Washington University, St. Louis, MO

Background
$\alpha_v\beta_3$-targeted paramagnetic nanoparticles permit molecular imaging of aortic vaso vasorum expansion in early atherosclerosis with MRI, and can simultaneously deliver targeted therapeutics. In this study, $\alpha_v\beta_3$-targeted nanoparticles detected and delivered fumagillin, a potent antiangiogenic compound, as well as assessed the extent of therapeutic success via MRI.
Methods
New Zealand White rabbits on a 1% cholesterol diet received $\alpha_v\beta_3$-targeted paramagnetic nanoparticles incorporating fumagillin (Targeted, n=4) or non-targeted nanoparticles (n=4). Black-blood MRI (1.5 T) of the abdominal aorta was performed before and four hours post nanoparticle injection. MRI was repeated one week post-treatement to assess angiogenesis in the vaso vasorum.
Results
At treatment, MRI enhancement was significantly higher with $\alpha_v\beta_3$-targeted than non-targeted nanoparticles (Figure, † $p < 0.05$). One week after treatment, MRI enhancement was significantly lower in $\alpha_v\beta_3$-targeted rabbits compared to non-targeted (Figure, * $p < 0.05$).
Conclusions
$\alpha_v\beta_3$-targeted nanoparticles sensitively detected angiogenesis within the vaso vasorum of atherosclerosic rabbits. Simultaneous targeted delivery of fumagillin significantly decreased the extent of neovasculture. These results suggest that MR molecular imaging with targeted perfluorocarbon nanoparticles provides a unique tool to detect early disease, to locally deliver effective treatment, and to assess therapeutic response.